JOURNAL OF AIRCRAFT
Vol. 39, No. 1, January–February 2002

Computational and Experimental Investigation of Limit Cycle Oscillations of Nonlinear Aeroelastic Systems

Essam F. Sheta* and Vincent J. Harrand†
CFD Research Corporation, Huntsville, Alabama 35805
and
David E. Thompson‡ and Thomas W. Strganac§
Texas A&M University, College Station, Texas 77843

A wide variety of pathologies, such as store-induced limit-cycle oscillations, have been observed on high-performance aircraft and have been attributed to transient nonlinear aeroelastic effects. Ignoring the nonlinearity of the structure or the aerodynamics will lead to inaccurate prediction of these nonlinear aeroelastic phenomena. The current paper presents the development and representative results of a high-fidelity multidisciplinary analysis tool that accurately predicts limit-cycle oscillations (LCOs) of an aeroelastic system with combined structural and aerodynamic nonlinearities. Wind-tunnel measurements have been carried out to validate the findings of the investigation. The current investigation concentrates on the prediction of the critical physical terms that dominate the mechanism of LCO. The aeroelastic computations predict LCO amplitudes and frequencies in very close agreement with the experimental data. The results emphasize the importance of modeling the nonlinearities of both the fluid and structure for the accurate prediction of LCO for nonlinear aeroelastic systems.

Nomenclature

a	=	nondimensional distance (in terms of b) from midchord to elastic axis
b	=	semichord of wing
c_h	=	viscous damping coefficient in plunge motion
c_α	=	viscous damping coefficient in pitch motion
I_{EA}	=	mass moment of inertia about elastic axis
k_h	=	structural stiffness coefficient in plunge motion
k_α	=	structural stiffness coefficient in pitch motion
m_c	=	mass of cam
m_t	=	total mass of system
m_w	=	mass of wing
r_c	=	nondimensional distance between elastic axis and cam center of rotation
r_{cg}	=	distance between elastic axis and center of mass
μ_h	=	structural damping coefficient in pitch motion
μ_α	=	structural damping coefficient in pitch motion

Introduction

AEROELASTIC problems represent a mutual interaction between the aerodynamics and structure of an aerospace vehicle. Several studies have established that aeroelastic systems are inherently nonlinear and that these nonlinearities lead to pathologies such as twin-tail buffet[1] and store-induced flutter and limit-cycle oscillations (LCO)[2] of fighter aircraft. These nonlinear aeroelastic problems are not accurately simulated by linear models. The design of a new generation of high-performance aircraft will depend primarily on the accurate prediction, understanding, and control of the critical physical terms that dominate the mechanism of nonlinear aeroelastic phenomena.

LCOs, in particular, have been a persistent problem on several fighter aircraft designs and are generally encountered on external store configurations. Bunton and Denegri[3] discuss LCO instabilities experienced during flight tests of the F-16 and F-18 aircraft. Denegri[4] further elaborates on extensive LCO experiences of the F-16 aircraft with external stores through analysis and flight tests. Stearman et al.[5] discuss flight-test data of LCO of an aircraft with various store configurations. Many nonlinear features are evident beyond the characteristic LCO. Denegri and Cutchins,[2] and Chen et al.[6] observed evidence of spring-hardening-type nonlinearity in the F-16 wing torsional stiffness. LCO was also observed as low as $M = 0.6$ at high angles of attack, and it was found to be sensitive to the tip missile configuration. O'Neil and Strganac[7] compare analytical predictions to experimental measurements for continuous nonlinear stiffening behavior in the pitch mode. The existence of torsion stiffness nonlinearities is found to induce LCO, which is dependent on velocity and the nonlinear parameters. Woolston et al.[8] investigated the effects of hysteresis and cubic stiffness nonlinearities on the flutter characteristics. The instabilities exhibited LCO due to cubic hardening only. In a related nonlinear phenomenon (see Jacobson et al.[9]), the B-2 exhibits residual pitch oscillations (RPOs) due to fluid–structure interaction that couple a flexible-body mode with a rigid-body mode.

The phenomenon is baffling because it appears over a broad range of Mach numbers ($0.6 < M < 1.1$), exhibits hysteresis with respect to onset and departure, may be maneuver and/or angle-of-attack dependent, and is configuration dependent. Regardless, store-induced LCO significantly restricts mission performance because LCO-induced accelerations lead to unacceptable loading for both the pilot and structure. The mechanism that leads to these LCOs is not well understood, but possible explanations under study by the community include aerodynamic and/or structural nonlinearities. Such nonlinearities may arise from structural dynamics/kinematics, oscillating shock or shock-induced flow separations, or nonlinear damping mechanisms. The signature of these observations suggests that the pathology will lead to LCO behavior similar to that investigated herein.

An extensive review of the analysis of structural nonlinearities for a wing section such as discussed in this paper may be found by Lee et al.[10] Analytical studies of systems with continuous nonlinear structural stiffness, such as those exhibited by the response of

Received 18 May 2000; revision received 15 February 2001; accepted for publication 20 March 2001.

*Senior Engineer, Software Technology Division. Member AIAA.
†Director/Software Technology, Software Technology Division. Member AIAA.
‡Graduate Research Assistant, Department of Aerospace Engineering. Student Member AIAA.
§Associate Professor, Department of Aerospace Engineering. Associate Fellow AIAA.

helicopter rotor systems, have been addressed by several researchers (see Tang and Dowell,[11] Woolston et al.,[8] Lee and LeBlanc,[12] and Price et al.[13]).

As an example of the ongoing experiences by the community, the following observations from ground- and flight-test measurements of LCOs on the F/A-18, taken from R. Yurkovich's panel discussion, "Limit Cycle Oscillation and Related Nonlinear Phenomena in Aircraft" at the 41st AIAA Structural Dynamics and Materials Conference in April 2000, are reviewed:

1) Stiffness tests show evidence of spring-hardening-type nonlinearity in the wing torsional stiffness, and measurements show that the wing behaves differently for leading-edge down vs leading-edge up.

2) The unsteady wing pressure (and accelerometer) data show a harmonic at about two times the LCO frequency, but there are no structural modes at this frequency.

3) Pylon pitch frequency is slightly below the wing bending frequency, and it is sensitive to damping. A lateral fuselage bending mode was involved in some cases.

4) The linear flutter mechanism is antisymmetric and involves pylon pitch coupling with wing bending. Although linear analysis predicts flutter for critical stores and store combinations, in reality, LCOs occur at a speed somewhat below the predicted linear flutter speed.

5) The LCO is sensitive to angle of attack (AOA). As AOA is increased either positive or negative, LCOs occur if the flight conditions are high enough.

6) LCO occurs in the transonic speed range for Mach numbers less than one, perhaps as low as $M = 0.7$, at elevated AOA.

7) From flight-test observations, the LCO is sensitive to the tip missile configuration. If the tip missile AOA is changed, the occurrence of LCO will change.

8) The mode shape during LCO in flight does not appear as conventional bending–torsion flutter. Torsion is almost in-phase with bending, and the maximum amplitude is at the trailing-edge tip.

These results are similar to those experiences of LCO behavior found for the F-16 as discussed by both Denegri[4] and Chen et al.[6] Furthermore, Cole[14] observed an aeroelastic behavior similar to that found in the LCO response of store configurations. The observed vibration characteristics suggested the presence of internal resonance. Internal resonance occurs as a result of nonlinearities that couple modes of motion of the system. The nonlinear coupling of the modes leads to an exchange of energy between the modes of the system as the natural frequencies become commensurable. The internal resonance is characterized by periodic amplitude modulation. The amount of energy that is exchanged depends on the type of nonlinearity and the relationship of the linear natural frequencies. Internal resonance is not predictable with linear analysis (see Nayfeh and Mook[15] and Nayfeh and Balachandran[16]). Oh et al.[17] examine response characteristics of a system dynamically similar to Cole's[14] experiment, but these studies are performed in the absence of aerodynamic loads. The results suggest that a two-to-one internal resonance is responsible for the instability because the frequency of the second bending mode is twice the frequency of the first torsional mode. Results show that an antisymmetric vibration mode may be indirectly excited by a two-to-one internal resonance mechanism.

Some recent efforts attempt to characterize nonlinear aeroelastic response. Denegri and Cutchins[2] discuss nonlinear behavior in aeroelastic systems and delineate their efforts to qualify nonlinear aeroelastic behavior using linear analysis. Denegri[4] (F-16) and Yurkovich (F-18, reviewed in the Introduction) both used traditional linear approaches to examine store-induced LCOs. Both have limited success because it appears that store-induced LCOs may be related to hump (or soft crossing) modes found in velocity-damping diagrams. In particular, linear theory might track frequencies associated with lightly damped modes identified with the store-induced LCOs; unfortunately, linear theory does not provide reliable or consistent response characteristics in many cases. Thus, it is felt (see Denegri[2]) that a nonlinear flutter analysis method is needed to capture fully the features and, more importantly, to provide reliable resources for certification and flight testing.

In this paper, experimental measurements of LCOs for a simple nonlinear aeroelastic system are conducted, and a high fidelity multidisciplinary computational environment (MDICE) is used to predict transient LCO behavior of this nonlinear aeroelastic system. MDICE has been developed by CFD Research Corporation in collaboration with U.S. Air Force Research Laboratory (AFRL). MDICE provides an environment in which several engineering analysis programs run concurrently and cooperatively to perform a multidisciplinary design, analysis, or optimization problem. The computational results are compared with experimental data. The investigation covers a wide range of flight conditions to give more insight on the parameters that dominate LCO of nonlinear aeroelastic systems.

LCO of Nonlinear Aeroelastic System

In this section, the experimental apparatus of this study is discussed and the particular set of analysis modules used in MDICE for the prediction of LCO of a simple nonlinear aeroelastic system is presented.

Nonlinear Aeroelastic Test Apparatus (NATA)

The experimental system that serves as the testbed for experimental investigations and validation of the numerical predictions of the nonlinear LCO is shown in Fig. 1. A model support system has been developed to provide direct measurements of nonlinear aeroelastic responses.[7] The support system permits prescribed pitch and plunge motion for a mounted wing section. The plunge motion is provided by a carriage that translates freely. Pitch motion is provided by a rotational cam mounted on this carriage. Large AOA are permitted, but protective constraints limit the amplitude of motion to prevent model/tunnel damage from large-amplitude LCOs.

The model support system provides freedom in test conditions and parameters. The structural stiffness response of the apparatus is governed by a pair of cams that are designed to provide tailored linear or nonlinear stiffness response. The shape of each cam, stiffness of the springs, and pretension in the springs dictate the nature of the nonlinearity. With this approach, these cams provide a large family of prescribed responses. Other physical properties, such as the eccentricity, the moment of inertia of the wing, the stiffness characteristics, and the wing shape, are easily modified for parametric investigations. System response is measured with accelerometers and optical encoders mounted to track motion in each degree of freedom.

Nonlinear Aeroelastic Model

The nonlinear aeroelastic system shown in Fig. 1 is modeled using the two-degree-of-freedom model shown in Fig. 2. The nonlinear equations of motion that prescribe the aeroelastic response of the described aeroelastic system are given by

$$m_t\ddot{h} + [m_w x_\alpha b\cos(\alpha) - m_c r_c b\sin(\alpha)]\ddot{\alpha} + c_h\dot{h} + [-m_w x_\alpha b\sin(\alpha) - m_c r_c b\cos(\alpha)]\dot{\alpha}^2 + k_h(h)h = -L(t) - \mu_h m_t g(|\dot{h}|/\dot{h}) \quad (1)$$

$$I_{EA}\ddot{\alpha} + [m_w x_\alpha b\cos(\alpha) - m_c r_c b\sin(\alpha)]\ddot{h} + c_\alpha\dot{\alpha} + k_\alpha(\alpha)\alpha = M(t) - \mu_\alpha M_f(|\dot{\alpha}|/\dot{\alpha}) \quad (2)$$

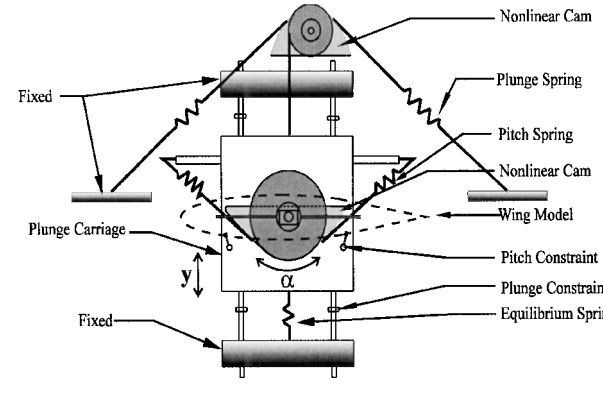

Fig. 1 Schematic view of NATA.

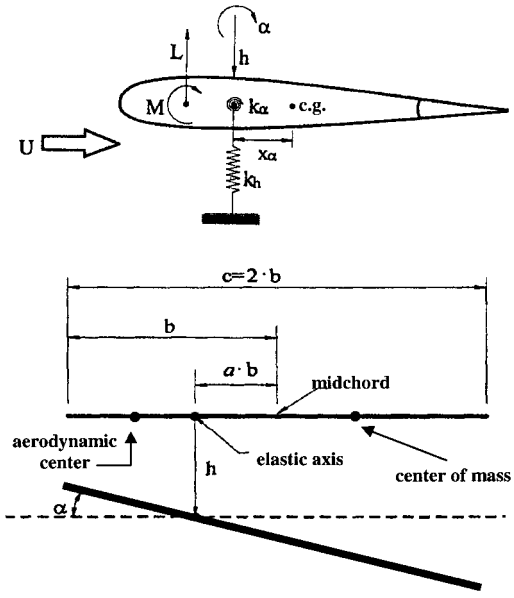

Fig. 2 Aeroelastic structure model with pitch and plunge degrees of freedom.

where m_t is the total mass of the wing and its support structure and m_w is the mass of the wing only. The elastic axis location a is nondimensionalized with respect to the half-chord length b and is positive for the elastic axis located aft of the midchord. In these equations, r_c represents the nondimensional distance between the elastic axis and the center of rotation of the cam and c_h and c_α are plunge and pitch viscous damping coefficients, respectively. The mass moment of inertia about the elastic axis I_{EA} is the contribution of the wing, cams, and the offset masses and is given by

$$I_{\text{EA}} = I_{w_{\text{cg}}} + I_{c_{\text{cg}}} + m_c(r_c b)^2 + m_w(x_\alpha b)^2 \tag{3}$$

Structural stiffnesses are represented by k_h and k_α for plunge and pitch motions, respectively. The last terms in the right-hand side of Eqs. (1) and (2) represent the coulomb structural damping, where M_f is the frictional moment and μ_α and μ_h are the structural damping coefficients in pitch and plunge motions, respectively.

The aerodynamic forces are represented by the normal force L and the pitching moment M. The aerodynamic forces are computed by solving the full Navier–Stokes equations. The aerodynamic forces are referenced to the elastic axis, and they are dependent on the motion of the wing. In general, solving the Navier–Stokes equations might be necessary to account for the aerodynamic nonlinearities of the system that may arise from viscosity effects, high-angle-of-attack aerodynamics, oscillating shocks, shock-induced flow separation, shock/boundary-layer interaction, vorticity evolution, and shedding. The cases considered in this investigation are shock free. However, the other sources of aerodynamic nonlinearities may exist.

The developed aeroelastic module incorporates various sources of nonlinearities, in addition to the aerodynamic nonlinearities. These nonlinear features include coulomb structural damping, nonlinear stiffness, and higher-order kinematics. For example, the nonlinear torsional stiffness of this aeroelastic module is realized by nonlinear cams. The nonlinear pitch spring stiffness is measured, and fifth-order polynomial approximation of the stiffness is assumed in the form

$$k_\alpha(\alpha) = k_{\alpha_0} + k_{\alpha_1}\alpha + k_{\alpha_2}\alpha^2 + k_{\alpha_3}\alpha^3 + \cdots \tag{4}$$

The actual coefficients in the polynomial representation of the spring stiffness are obtained from measured displacements and loads. The even-order terms of Eqs. (4) exist to model the asymmetry in the stiffness of the torsional spring. The coefficients of the polynomial equation are given in Table 1 along with the other physical parameters and characteristics of the aeroelastic system. The computed

Table 1 Physical parameters of the nonlinear aeroelastic system

Parameter	Value
m_t	12.0 kg
m_w	1.662 kg
m_c	0.718 kg
b	0.1064 m
span	0.6 m
a	−0.4
r_{cg}	$(0.82 \times b - b - a \times b)$ m
I_{EA}	$0.04325\,\text{kg}\cdot\text{m}^2 + m_w \cdot r_{\text{cg}}^2$
r_c	1.1936
k_h	2844.4 N/m
k_α	$6.861422(1 + 1.1437925\alpha + 96.669627\alpha^2 + 9.513399\alpha^3 - 727.664120\alpha^4)$ N · m/rad
c_h	27.43 kg/s
c_α	$0.036\,\text{kg}\cdot\text{m}^2/\text{s}$
μ_α	0.0113
μ_h	0.0221

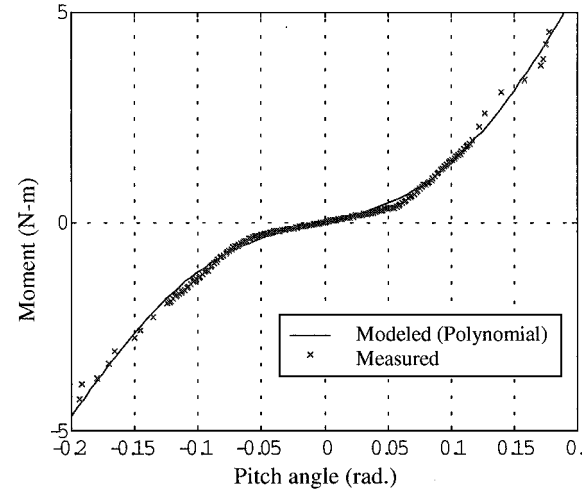

Fig. 3 Measured and modeled moment vs pitch angle of nonlinear pitch spring.

restoring moment vs the pitch angle, with the approximated polynomial stiffness, is compared very well with the measured restoring moment in Fig. 3. The aeroelastic equations (1) and (2) are integrated using a time marching finite difference routine based on the model introduced by Lee and LeBlanc.[12]

Fluid-Dynamics Module

The fluid-dynamics analysis module used for the current study is CFD-FASTRAN.[18] CFD-FASTRAN is a Reynolds-averaged full Navier–Stokes flow solver for modeling unsteady, turbulent flow problems using structured and/or unstructured grids. CFD-FASTRAN employs an upwind scheme with Roe's flux-difference splitting or Van Leer's flux-vector splitting for spatial differencing. Temporal differencing is done using a Runge–Kutta scheme, point-implicit scheme, or a fully implicit scheme. Turbulent models in CFD-FASTRAN include Baldwin–Lomax, $k-\varepsilon$, and $k-\omega$ models. CFD-FASTRAN also provides the state of the art for modeling flow problems with multiple moving bodies using chimera overset gridding methodology coupled with a six-degree-of-freedom model. The current simulation uses a fully implicit, finite volume scheme with Roe's flux-difference splitting and $k-\varepsilon$ turbulence model.

Grid Motion Technique

To carry out the computations, a C-type grid is generated around NACA-0015 airfoil (the airfoil section of the wing tested in the wind tunnel). The size of the computational grid is 300×40 grid cells with 200 grid cells on the airfoil surface. The far-field boundary extends to 10 chord lengths in all directions. A close-up view of the grid is shown in Fig. 4. At every time step, the grid is deformed due

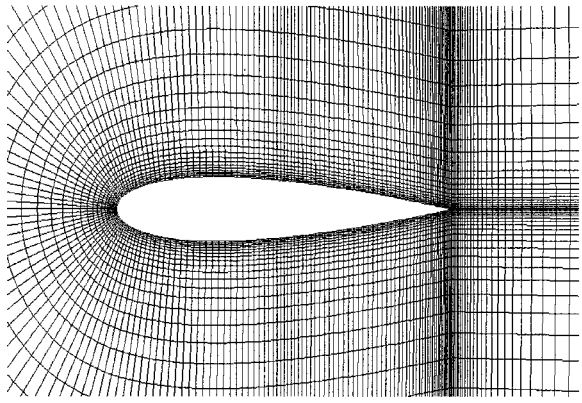

Fig. 4 C-type grid for NACA-0015 airfoil.

to the motion of the airfoil. The grid is deformed using transfinite interpolation functions (TFI). The advantages of using TFI are that TFI is an interpolation procedure that conforms to specified boundaries, and TFI is very computationally efficient.[19] The TFI routine is invoked automatically when the aerodynamic and aeroelastic data are exchanged between application modules.

MDICE Architecture

MDICE is a distributed object-oriented environment that is made up of several major components. The first component is a central controlling process that provides network and application control, serves as an object repository, carries out remote procedure calls, and coordinates the execution of several application programs via MDICE specific script language. The second component is a collection of libraries, each containing a set of functions callable by the application programs. These libraries provide low-level

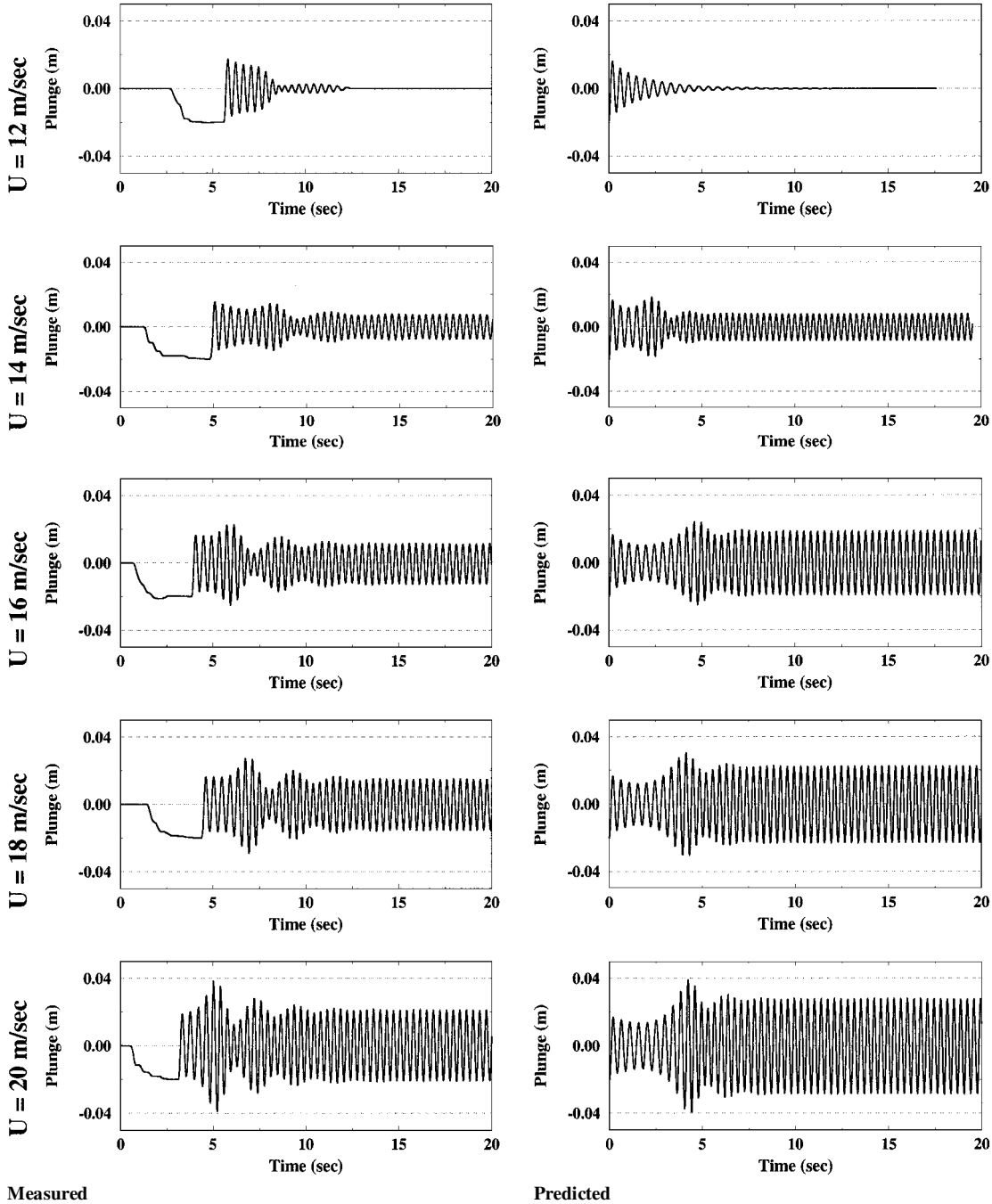

Fig. 5 Measured and predicted responses of plunge oscillations of nonlinear aeroelastic system at different freestream velocities.

communication and control functions that are hidden from the application programs, as well as more visible functionality such as object creation and manipulation, interpolation of flow data along interfaces, and safe dynamic memory allocation services. Finally, the environment also encompasses a comprehensive set of MDICE-compliant application programs. MDICE provides capabilities for parallel execution of participating application programs and has a full FORTRAN interface for those codes written in FORTRAN 77 or 90, C, in addition to C++. In a typical MDICE application, the application modules are selected, and the computer hosts used to execute the modules are chosen. Next, the application is run and controlled by MDICE using a short script in the graphical user interface that explicitly specifies the synchronization between the modules. The MDICE script contains all of the conveniences found in most common script languages. In addition, MDICE script supports remote procedure calls and parallel execution of the application modules. These remote procedure calls are the mechanism by which MDICE controls the execution and synchronization of the participating applications. Each application posts a set of available functions and subroutines. These functions are invoked from MDICE script, but are executed by the application program that posted the function.

There are many advantages to the MDICE approach. Using this environment, one can avoid giant monolithic codes that attempt to provide all needed services in a single large computer program. Such large programs are difficult to develop and maintain and by their nature cannot contain up-to-date technology. The MDICE allows the reuse of existing, state-of-the-art validated codes. The flexibility of exchanging one application program for another enables each engineer to select and apply the technology best suited to the task at hand. Efficiency is achieved by utilizing a parallel-distributed network of computers. Extensibility is provided by allowing additional engineering programs and disciplines to be added without modifying or breaking the modules or disciplines already in the environment. For more details of MDICE architecture, see Kingsley et al.[20]

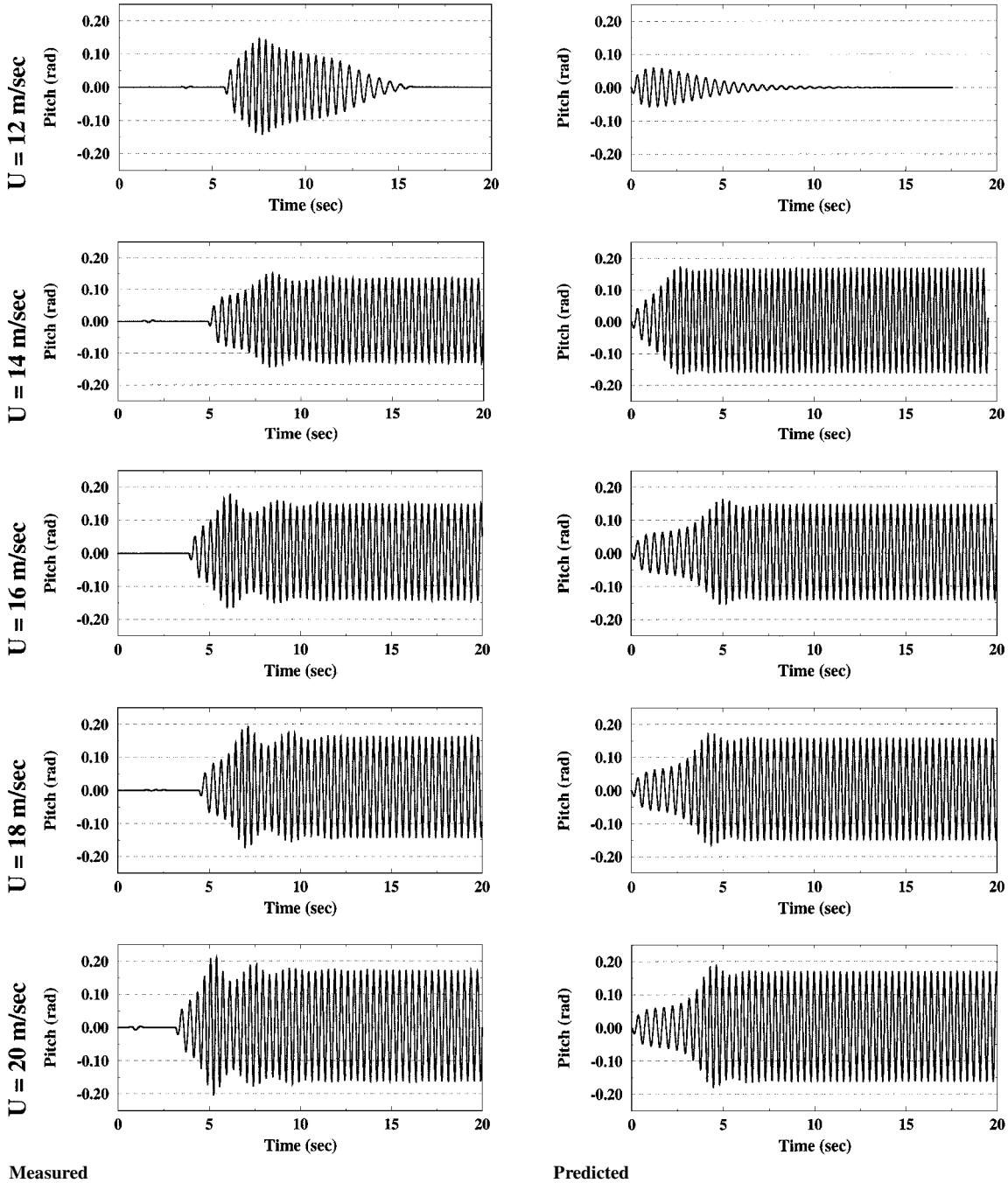

Fig. 6 Measured and predicted responses of pitch oscillations of nonlinear aeroelastic system at different freestream velocities.

Results and Discussion

The aeroelastic system is investigated subject to initial disturbance of displacements only, with no initial velocities. The experimental tests are conducted by setting the aeroelastic system at the initial conditions, waiting for few seconds until the fluctuations in the freestream velocity vanishes, then releasing the structure and monitoring the responses. All of the cases considered in this investigation are corresponding to an initial plunge displacement of −0.02 m. The effect of initial pitch displacement is investigated by O'Neil and Strganac.[7] The measured and predicted plunge and pitch responses at different freestream velocities are shown in Figs. 5 and 6, respectively. In the experimental data, the initial time of response of every case is different, depending on the releasing time of the structure. At a freestream velocity of 12 m/s, the system exhibits damped responses. At freestream velocities of 14 m/s and higher, the system clearly exhibits LCO responses. The wind-tunnel experiments showed that the system generally exhibits LCO for freestream velocities larger than 13 m/s (see O'Neil and Strganac[7]). LCOs continue over a large range of freestream velocities. The predicted pitch and plunge responses agree very well with the experimental data over a large range of velocities, especially for the pitch degree of freedom. Figures 5 and 6 also show that the LCO amplitude of pitch and plunge are slightly increased with the increase of freestream velocity.

The effect of freestream velocity on the LCO amplitude of pitch and plunge responses and the frequency of oscillations are shown in Fig. 7 for both the measured and predicted results. Figure 7 shows that the predicted results are in close agreement with the measured results. The LCO pitch amplitude has increased by about 0.012 rad and the LCO plunge amplitude has increased by about 0.0045 m for every 2 m/s increase in the freestream velocity. The frequency of oscillations changed very slightly over the range of freestream velocities considered. The average frequency is about 2.8 Hz. The small variation of the LCO responses and frequency over large range of freestream velocities indicates that the LCO shown are strongly dependent on the structural nonlinearity of the system. The dependence

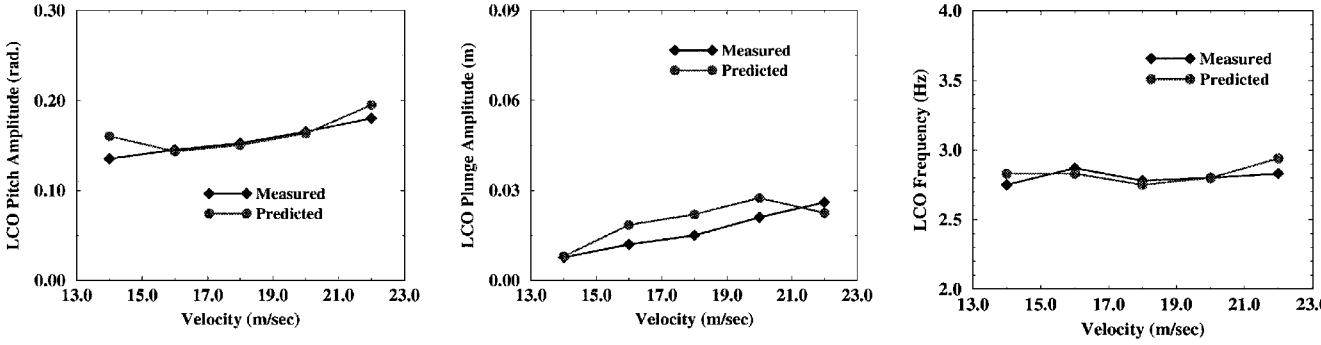

Fig. 7 Comparison of pitch and plunge LCO amplitude and LCO frequency between measured and predicted responses.

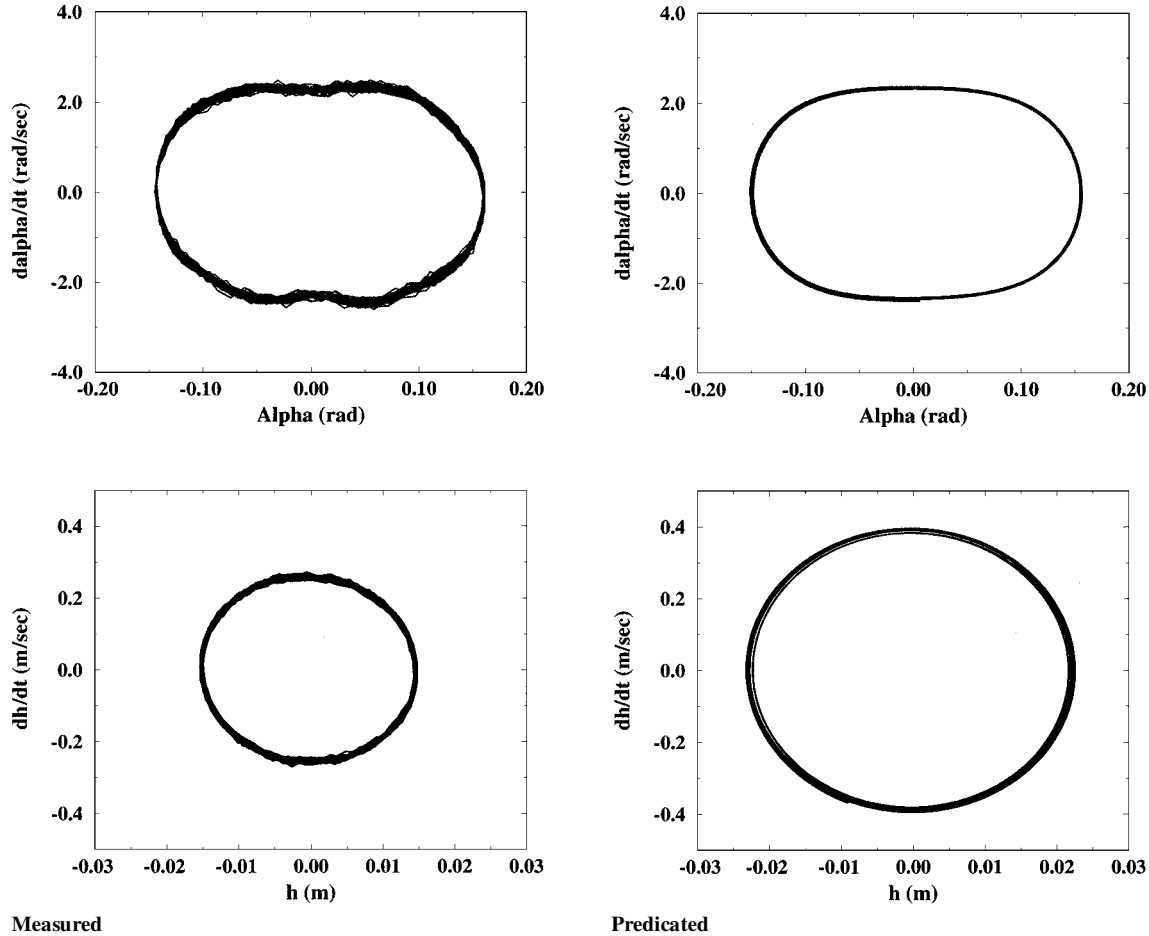

Fig. 8 Phase diagram of pitch and plunge LCO responses compared with measured responses at freestream velocity of $u = 18$ m/s.

of the structural responses on the aerodynamic nonlinearities will be emphasized later in the investigation.

A more detailed study for the case of the freestream velocity of 18 m/s is given in Figs. 8–16. Figure 8 shows the phase diagram (velocity vs displacement) of the pitch and plunge LCO responses for both the measured and predicted results. The LCO in both pitch and plunge is obvious, and they compare well with the measured data. The pitch oscillation exhibits LCO in the range of ±2.2 rad/s (predicted and measured) and the plunge oscillation exhibits LCO in the range of ±0.3 m/s for the measured results and ±0.4 m/s for the predicted results.

Figures 9 and 10 show the power spectral density (PSD) of the pitch and plunge LCO amplitudes and accelerations, respectively. The first peak shows that the predominant frequency of the nonlinear system is 2.78 Hz, and it is the same for both the plunge and pitch. The computational model has predicted very accurately the predominant frequency and the PSD peak of the pitch and plunge amplitudes and accelerations. Figure 10 shows that the nonlinear system exhibits another peak in the higher-order harmonics, and it is more significant in the pitch degree of freedom. The higher-order harmonics are indicative of the nonlinearity of the structural model. The computational model also predicted accurately this higher harmonic frequency and peak. In a separate study, Tang and Dowell[11] showed a comparison of experimental and analytical fast Fourier transform with higher-order harmonics caused by the structural nonlinearity of the system. Their primary frequency was over estimated by about 1 Hz. In their model, they used a linear unsteady aerodynamic model without stall. This is an indication of the importance of including the nonlinearity of the fluid flow instead of an analytical formulation of the unsteady aerodynamic forces. Thus, as indicated from Figs. 9 and 10, including the nonlinearity of the fluid as well as of the structure will result in capturing the frequency and peaks of the response, including the higher harmonics.

Thus, to give more insight about the effect of the whole system nonlinearity and different physical parameters on the nonlinear system response, the pitch and plunge responses are computed using different methodologies at a freestream velocity of 18 m/s and plunge initial condition of $h_{ic} = -0.02$ m. The results have been summarized in Figs. 11–16. The measured data corresponding to this case are shown in Figs. 5 and 6. In Fig. 11, the responses

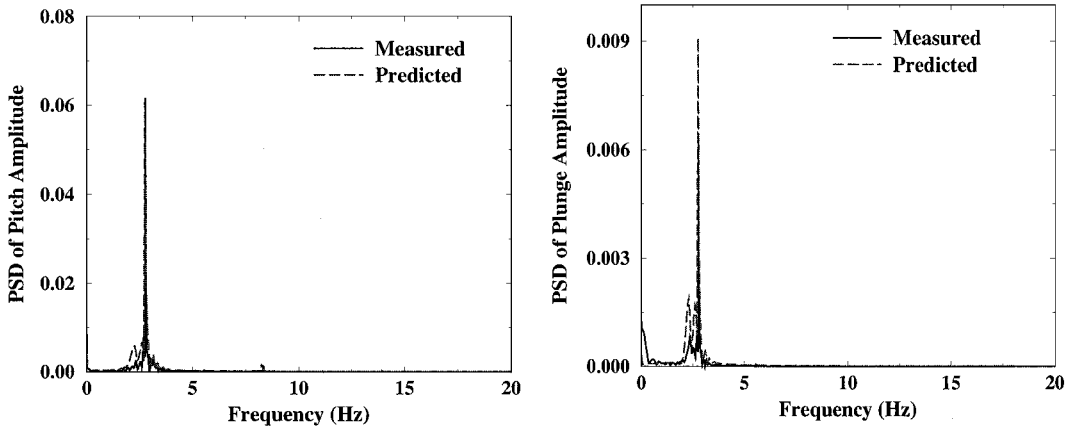

Fig. 9 PSD of pitch and plunge LCO amplitudes compared with measured data.

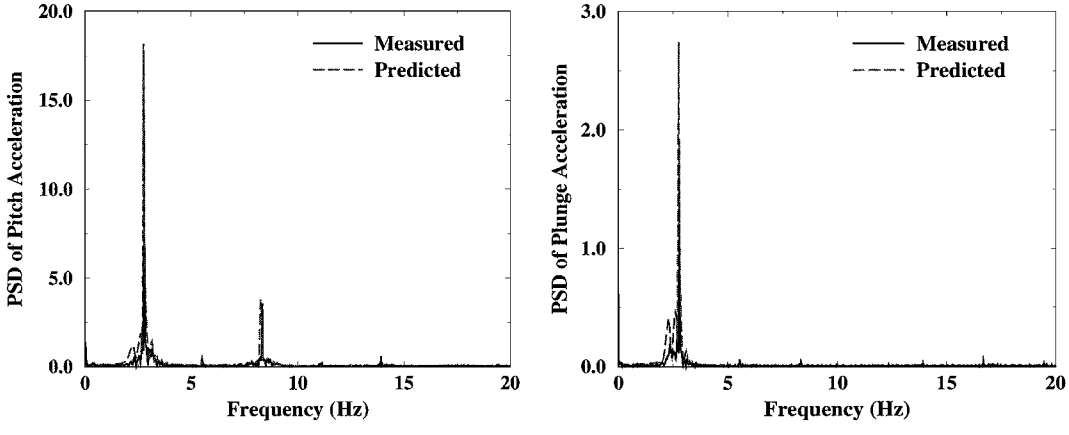

Fig. 10 PSD of pitch and plunge LCO accelerations compared with measured data.

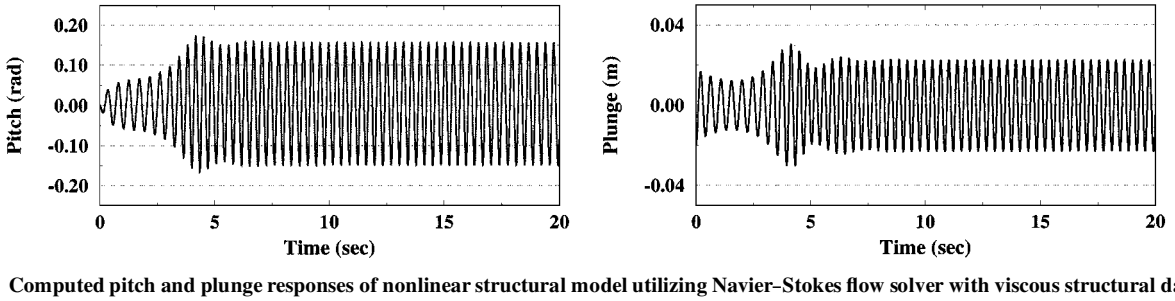

Fig. 11 Computed pitch and plunge responses of nonlinear structural model utilizing Navier–Stokes flow solver with viscous structural damping.

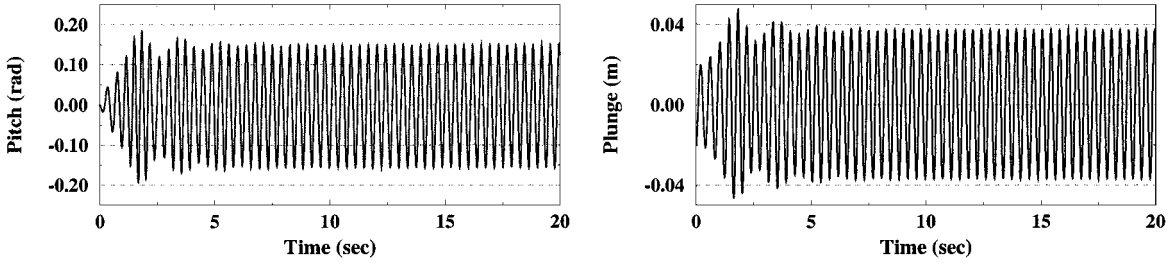

Fig. 12 Computed responses of nonlinear structural model utilizing quasi-steady Theoderson's linear aerodynamic model.[21]

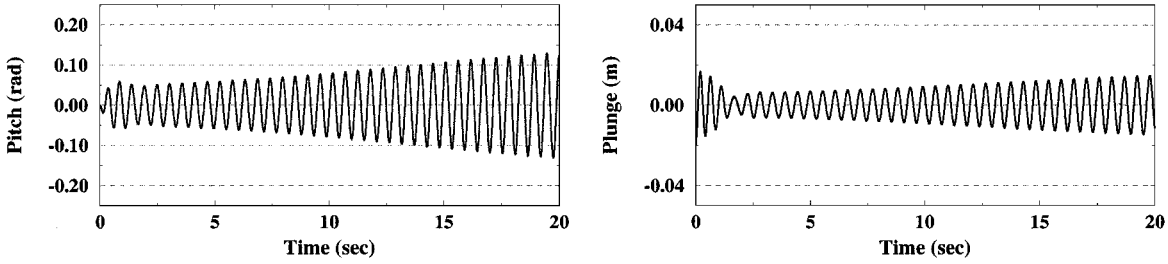

Fig. 13 Computed responses using linear structural model and utilizing Navier–Stokes flow solver.

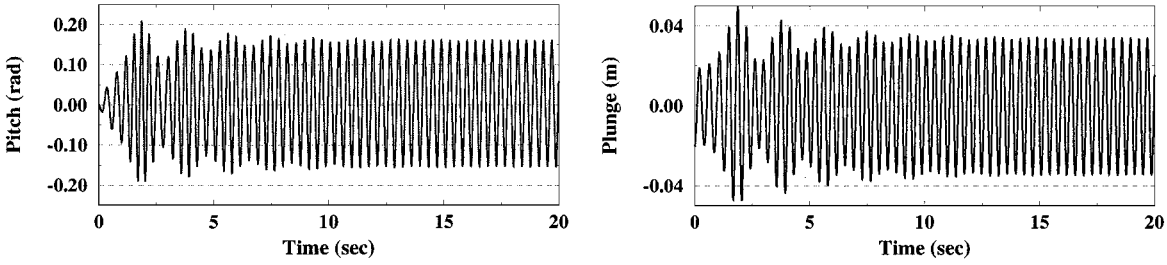

Fig. 14 Computed responses of nonlinear structural model with structural damping only and utilizing Navier–Stokes flow solver.

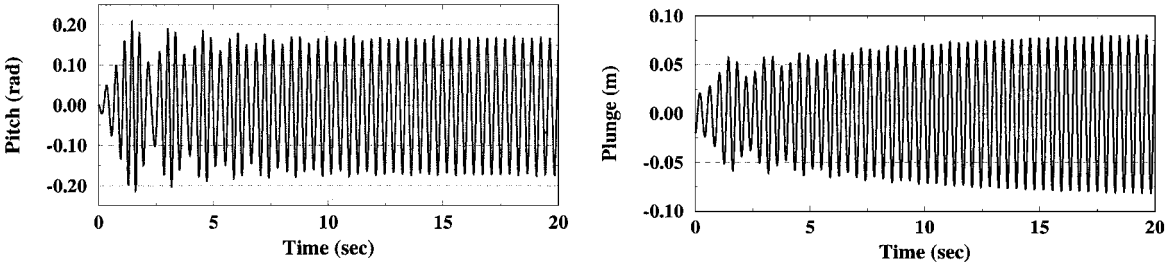

Fig. 15 Computed responses of nonlinear structural model with no damping and utilizing Navier–Stokes flow solver.

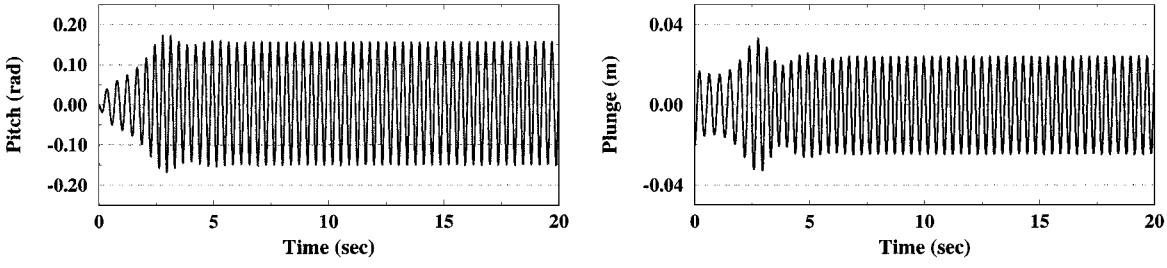

Fig. 16 Computed responses of nonlinear structural model and utilizing Euler flow solver.

are computed using a high-fidelity model utilizing Navier–Stokes flow solver and a nonlinear structural model with viscous damping to model the effect of flow viscosity on the structure. The results are in very close agreement with the measured data. The frequency of oscillations is predicted within 1% of the measured value. This model also captured the PSD peaks and frequencies efficiently as shown in Figs. 9 and 10.

In Fig. 12, the responses are computed using the nonlinear structural model and a quasi-steady linear aerodynamic model based on Theodorsen's theory.[21] This model is often effective to model aerodynamic forces for similar aeroelastic systems.[7,12] Although the nonlinear system exhibits LCO in both the pitch and plunge degrees of freedom, the amplitude of the plunge LCO is almost 2.6 times that of the measured amplitude. This is another indication that the LCO pathology is a phenomenon that is affected by both the fluid and structure nonlinearities. The use of an unsteady aerodynamics model (not shown) instead of a quasi-steady model did not change the results, probably because of the very low reduced frequency,

$k = 0.016$. In Fig. 13, the responses are computed using a high-fidelity Navier–Stokes flow solver and assuming a linear structural model. As expected, due to the extensive structural pitch nonlinearity of this system, the predicted responses are much smaller than the measured data, and they even show a slight increasing response. The frequency of oscillations is 1.82 Hz, which is 35% less than the measured value. Recall that the nonlinear structural model predicted the frequency within 1% of the measured value. In Figs. 14 and 15, the responses are computed using the same nonlinear structural model and using the Navier–Stokes flow solver. However, only structural damping is considered in computing the responses shown in Fig. 14, whereas no damping is considered in computing the responses shown in Fig. 15. In both cases, the results are much better than the low-fidelity models presented in Figs. 12 and 13. The pitch LCO is accurately predicted. However, the case of structural damping only produces a plunge LCO that is 2.25 times the measured value. The case of no damping is worse; the plunge LCO amplitude is 5.36 times the measured value. This is an indication of the importance of modeling the effect of viscous damping on the structural response even if the viscosity is modeled in the fluid-flow model. In Fig. 16, the responses are computed using the nonlinear structural model and Euler (inviscid) flow solver. The results show good agreement with the measured data. However, the plunge LCO amplitude is higher than both the measured value and the value computed using the Navier–Stokes flow model of Fig. 11. This shows the importance of modeling the effect of flow viscosity on the unsteady aerodynamic forces that directly affect the response of the structure. From Figs. 14–16, we conclude the importance of modeling the effect of flow viscosity in both the aerodynamic model and the structural-dynamics model. In the aerodynamics model, the viscosity is inherited in the Navier–Stokes solution model. In the structural-dynamics model, the damping effects of the flow viscosity are included in the viscous damping terms and they are represented by the coefficients c_h and c_α. The viscosity effects can not be modeled accurately if analytic aerodynamic formulations were used.

In summary, the results of this paper clearly indicate the importance of modeling all nonlinearities of the aeroelastic system. In addition, the physical characteristics of the aeroelastic system, such as damping and viscous effects, should also be modeled. Even though the cases considered in this paper are for low reduced frequency and in the low subsonic regime, the importance of a high-fidelity flow model is apparent. In cases of high reduced frequency, transonic flow, or shock/boundary-layer interaction, the importance of modeling the nonlinearity of the fluid and structure will be further emphasized.

Conclusion

Computational and experimental investigations are conducted to measure and accurately predict LCOs of a simple nonlinear aeroelastic system. Linear analysis of structure dynamics response and/or low-fidelity flow models fails to predict the LCO behavior of this nonlinear aeroelastic system. A high-fidelity analysis tool that models the nonlinearity of both the fluid and structure is developed and integrated into the MDICE. The computational results of this analysis tool predict LCO amplitudes and frequencies in very close agreement with the experimental data. The results indicated the importance of modeling the nonlinearities of both the fluid and structure for the accurate prediction of LCO of nonlinear aeroelastic systems.

Acknowledgments

This research work is sponsored by the U.S. Air Force Office of Scientific Research under a Small Business Technology Transfer Research program. The authors wish to acknowledge Brian Sanders and Daniel Segalman of U.S. Air Force Research Laboratory (AFRL) for his funding and support of the current work. The first two authors acknowledge Don Kinsey and Lawrence Huttsell of AFRL for their support of the multidisciplinary computing environment.

References

[1]Shah, G. H., "Wind-Tunnel Investigation of Aerodynamic and Tail Buffet Characteristics of Leading-Edge Extension Modifications to the F/A-18," AIAA Paper 91-2889, Aug. 1991.

[2]Denegri, C. M., and Cutchins, M. A., "Evaluation of Classical Flutter Analyses for the Prediction of Limit Cycle Oscillations," AIAA Paper 97-1021, April 1997.

[3]Bunton, R. W., and Denegri, C. M., Jr., "Limit Cycle Oscillation Characteristics of Fighter Aircraft," *Journal of Aircraft*, Vol. 37, No. 5, 2000, pp. 916–918.

[4]Denegri, C. M., Jr., "Limit Cycle Oscillation Flight Test Results of a Fighter with External Stores," *Journal of Aircraft*, Vol. 37, No. 5, 2000, pp. 761–769.

[5]Stearman, R. O., Powers, E. J., Schwartz, J., and Yurkovich, R., "Aeroelastic Identification of Advanced Technology Aircraft Through Higher Order Signal Processing," *Proceedings of the 9th International Modal Analysis Conference*, Society for Experimental Mechanics, Bethel, CT, 1991, pp. 1607–1616.

[6]Chen, P., Sarhaddi, D., and Liu, D., "Limit-Cycle-Oscillation Studies of a Fighter with External Stores," AIAA Paper 98-1727, 1998.

[7]O'Neil, T., and Strganac, T. W., "Aeroelastic Response of a Rigid Wing Supported by Nonlinear Springs," *Journal of Aircraft*, Vol. 35, No. 4, 1998, pp. 616–622.

[8]Woolston, D. S., Runyan, H. L., and Andrews, R. E., "An Investigation of Effects of Certain Types of Structural Nonlinearities on Wing and Control Surface Flutter," *Journal of the Aeronautical Sciences*, Vol. 24, No. 1, 1957, pp. 57–63.

[9]Jacobson, S. B., Britt, R. T., Dreim, D. R., and Kelly, P. D., "Residual Pitch Oscillation (RPO) Flight Test and Analysis on the B-2 Bomber," AIAA Paper 98-1805, April 1998.

[10]Lee, B. H. K., Price, S. J., and Wong, Y. S., "Nonlinear Aeroelastic Analysis of Airfoils: Bifurcation and Chaos," *Progress in Aeronautical Sciences*, Vol. 35, No. 3, 1999, pp. 205–335.

[11]Tang, D. M., and Dowell, E. H., "Comparison of Theory and Experiment for Non-Linear Flutter and Stall Response of a Helicopter Blade," *Journal of Sound and Vibration*, Vol. 165, No. 2, 1993, pp. 251–276.

[12]Lee, B. H. K., and LeBlanc, P., "Flutter Analysis of a Two-Dimensional Airfoil with Cubic Nonlinear Restoring Force," *Aeronautical Note-36*, National Research Council (Canada) No. 25438, Ottawa, Ontario, Canada, 1986.

[13]Price, S. J., Aliganbari, H., and Lee, B. H. K., "The Aeroelastic Response of a Two-Dimensional Airfoil with Bilinear and Cubic Structural Nonlinearities," *Journal of Fluids and Structures*, Vol. 9, No. 2, 1995, pp. 175–193.

[14]Cole, S. R., "Effects of Spoiler Surfaces on the Aeroelastic Behavior of a Low-Aspect-Ratio Wing," AIAA Paper 90-0981, April 1990.

[15]Nayfeh, A. H., and Mook, D. T., *Nonlinear Oscillations*, Wiley, New York, 1979, pp. 26–34.

[16]Nayfeh, A. H., and Balachandran, B., "Modal Interactions in Dynamical and Structural Systems," *Applied Mechanics Review*, Vol. 42, No. 11, Pt. 2, 1989, pp. S175–S201.

[17]Oh, K., Nayfeh, A. H., and Mook, D. T., "Modal Interactions in the Forced Vibrations of a Cantilever Metallic Plate," *Nonlinear and Stochastic Dynamics*, Vol. 78, American Society of Mechanical Engineers, Fairfield, NJ, 1994, pp. 237–247.

[18]*CFD-FASTRAN User's Manual*, Theory Manual, Ver. 2.2, CFD Research Corp., Huntsville, AL, 1998, pp. 1.1–1.6.

[19]Thompson, J. F., Soni, B. K., and Weatherill, N. P., *Handbook of Grid Generation*, CRC Press, Boca Raton, FL, 1998, pp. 3.1–3.15.

[20]Kingsley, G. M., Siegel, J. M., Harrand, V. J., Lawrence, C., and Luker, J., "Development of the Multidisciplinary Computing Environment (MDICE)," AIAA Paper 98-4738, Sept. 1998.

[21]Theodorsen, T., "General Theory of Aerodynamic Instability and the Mechanism of Flutter," NACA Rept. 496, 1935.